CITATION: M. Irfan et al., "An IoT-Based Noncontact ECG System: Sole of the Feet/Hands Palm," in IEEE Internet of Things Journal, vol. 10, no. 21, pp. 18718-18732, 1 Nov.1, 2023, doi: 10.1109/JIOT.2023.3283037

which has been published in final form at

DOI: http://dx.doi.org/10.1109%2FJIOT.2023.3283037

An IoT-Based Non-Contact ECG System: Sole of the Feet / Hands Palm

Muhammad Irfan, Peng Shun, Barkoum Betra Felix, Noman Mustafa, Saadullah Farooq Abbasi, Abdelwahed Nahli, Abdulhamit Subasi, Tomi Westerlund *Senior member, IEEE,* Wei Chen *Senior member, IEEE,*

***Abstract*—In smart healthcare facilities designed especially for the elderly, non-contact electrocardiogram (ECG) measurements could provide essential information about an elderly person's health by enabling long-term health analytics. In this research work, we propose an Internet of Things (IoT) based non-contact ECG measurement system. The non-contact measurement is done using flexible electrodes that are made of fabric. These fabric-based flexible electrodes are designed to measure ECG signals from the sole of the feet (SOF) or the palms of the hands (POH) without touching human skin. To mitigate the impact of nearby electromagnetic radiation on the electrodes, a double layer of isopotential shielding is placed underneath the two active electrodes. The gathered biosignals are stored in the IoT device and transmitted to the cloud. To reduce the amount of stored and transmitted data, we improved our adaptive coding algorithm. The adaptive coding results in an average data reduction of 72%. The data can be fully recovered in the cloud for further analyses using advanced cloud-based tools in ThingSpeak. The study tested the proposed system on 35 participants, including elderly persons, adults, and children. Based on the experiments, the proposed system accurately measures the ECG signal. We validated the results with the ground truth data (polysomnography (PSG)) showing an average heart rate (HR) error of ∓ 1 beat per minute (BPM). Moreover, we compared QRS complexes detected on wrists with those detected from SOF (with or without socks), POH (with or without gloves), and one hand and one foot (with or without a sock and glove), and found no significant differences.**

***Index Terms*—ECG, non-contact, flexible electrodes, feet soles, socks, hand palms, gloves, adaptive coding, Internet of Things (IoT).**

I. Introduction

THE demand for personalized healthcare systems (PHS) is rising since there are approximately 727 million elderly people and 1 billion disabled individuals [1], [2]. Disability affects nearly everyone at some point in their lives, and in fact, 15% of the world's population has a disability, a number that is growing due to aging and noncommunicable diseases [3]. The report compiled by the World Health Organization (WHO) in 2011 highlights some significant statistics, including 75 million people (or 1% of the global population) use wheeled mobility every day, which is more than twice as many as Canadians [1]. Moreover, the elderly population is projected to grow 56% between 2015 and 2030, from 901 million to 1.4 billion and it is expected to double by 2050 (to approximately 2 billion) [2], [4]. Additionally, older people are more likely to be disabled because of the cumulative effects of diseases, injury, and chronic illness. This contributes to the higher rates of disability among the elderly. For these people, the importance of the PHS is evident.

Health Internet of Things (IoT) nodes as part of the PHS has the potential to decrease healthcare costs and increase revenue by more than $300 billion in the United States each year [5]. These sensors can also be installed in living spaces to monitor and assist senior citizens in regaining their mobility while making sure appropriate medical care is provided [6], [7]. It is possible to connect these sensors to home monitoring devices, which can then be connected to hospital monitoring systems. This can help gather, process, monitor, and transfer valuable information across multiple environments [8]. IoT also offers the possibility of connected scales or wearable heart monitors as tools for encouraging healthy living [9].

As part of the IoT, the Internet of Medical Things (IoMT) facilitates medical services for the disabled, the elderly, and those in remote locations. Technology can be adapted to accommodate the specific needs of different users, such as alert notifications sent to family members or providing remote medical monitoring [10]–[15].

IoMT sensors are extremely low-cost and easily disposable due to advances in plastics and fabrics. Using these sensors combined with radio frequency identification (RFID) electronics, it is possible to manufacture wireless-powered disposable sensing devices on paper or e-textiles [16]. Now doctors, nurses, patients, family members, and others can access patient information in the form of medical records stored in a database using IOMT. This makes it easy for doctors to access patient information [16]. Additionally, IoT-based systems are patient-centric, meaning they respond to patients' medical conditions. Health IoT technology plays a key role in preventing and controlling chronic diseases. Through wireless connectivity, healthcare practitioners can collect and analyze patient data as well as perform remote monitoring [17]–[19].

Muhammad Irfan is with Center for Intelligent Medical Electronics (CIME), Fudan University, China, and with the Faculty of Technology, University of Turku (UTU), Finland (imuhammad18@fudan.edu.cn). Wei Chen (corresponding author) is a director of CIME group at Fudan University, China (w_chen@fudan.edu.cn). Peng Shun is with Huawei, Shanghai, China. Barkoum Betra Felix is with Paul Sabatier University, France (felix.barkoumbetra@univ-tlse3.f). Noman Mustafa is with Optical Instruments China (noman_mustafa@sjtu.edu.cn). Abdelwahed Nahli is with Fudan University (nabdelwahed21@m.fudan.edu.cn). Saadullah Farooq Abbasi is with Riphah Interna-tional University Islamabad, Pakistan (su.farooq@riphah.edu.pk). Abdulhamit Subasi is with the Faculty of Medicine, UTU, Finland, and with the College of Engineering, Effat University, Saudi Arabia, (abdulhamit.subasi@utu.fi). Tomi Westerlund is with the Faculty of Technology, at UTU, Finland (tovewe@utu.fi).

This work is supported by Shanghai Municipal Science and Technology International R& D Collaboration Project (Grant No. 20510710500) and Shanghai Municipal Science and Technology Major Project (Grant No. 2017SHZDZX01).

Main Contributions and Novelty: The goal of monitoring physiological signals without direct contact and at home is to reduce invasiveness, increase comfort, and enhance the quality of life. At the same time, we need to ensure high-quality data to reliably assess the health of an elderly person. Our proposed system will allow elderly persons to benefit from greater convenience and quicker responses with the help of the IoT. The main contributions of the article are:

1) A non-contact ECG design to monitor heart rate (HR) and electrocardiogram (ECG) from the sole of feet (SOF) with socks
2) HR and ECG signals from the palms of the hands (POH) with gloves
3) ECG signal is recorded with a glove on one hand palm and with a sock on a foot sole
4) Optimized cloud data transmission without sacrificing accuracy through adaptive coding

The paper is structured as follows. Section II discusses the relevant work. Section III explain the design of the system, electrode material, electrode placement, and hardware design. Section IV presents details on the dual-slope, adaptive coding algorithm, and cloud services. Section V discusses the experimental setup, data collection process, and results of the proposed system. Furthermore, a Polysomnography (PSG) device is used as a ground truth to validate the ECG signals measured by the proposed system. Section VI contains a discussion, followed by Section VII, in which the work is concluded.

II. Related Work

A common cause of pain and even death is heart disease [20]. The monitoring of cardiac signals can aid in the diagnosis and prevention of cardiovascular diseases in the early stages [21], [22]. Conventional ECG measurement systems have many limitations that the proposed system will solve with non-contact measurements. One of the limitations of contact-based measurements is that a gel on a silver/silver chloride (Ag/Agcl) dries out over time, deteriorating the signal quality. Another one is that wet electrodes may not be appropriate for prolonged ECG measurements, since they may cause discomfort, skin irritation, and inflammation, particularly in patients who are prone to allergic reactions [23]. This could potentially lead to less accurate measurements. In addition, often when skin is injured, electrodes cannot be placed directly on the body.

In recent years, dry electrodes have been studied more and more in the field of ECG measurements, as they are capable of making ECG measurements without subject awareness. Researchers have proposed some multi-parameter devices. Certain sensing devices, such as electronic bathroom scales, can measure different physiological signals synchronously and in a contacting manner [24], [25], and a handheld device [26]. Long-term periodic measurements are convenient to take at home without professional assistance. Physiological signals, like the ECG and Impedance Plethysmography (IPG), are normally recorded on dry electrodes with metal plates, but they should ensure a steady $ohmic$ connection with the skin. Contrary to this, many bio-potential signals can be recorded using non-contact electrodes. Non-contact approaches can avoid electrode contact's negative effects such as irritation and discomfort [27], [28]. The flexible electrode consists of a silver fibre conductive fabric (SFCF), which allows physiological signals to be acquired (e.g. ECG) without contact. These electrodes have the ability to detect bio-potential signals through the gap between the sensor and the human body. It offers comfort; however, it is susceptible to electromagnetic radiation interference due to the larger electrode area. To suppress the influence of nearby electromagnetic radiation on the electrodes, a double layer of iso-potential shielding is placed underneath the two active electrodes.

A growing number of the elderly are suffering from cardiovascular diseases, and therefore it is essential to have a system empowering the elderly to measure physiological signals at home. The invention of the IOMT makes this possible. It provides remote monitoring and multi-patient monitoring, reducing the number of hospital visits and providing regular feedback. IoT-based systems, however, rely on Wi-Fi for transmitting data packets to cloud servers, consuming more power than other technologies, such as Bluetooth [29]. Also, some cloud services are free, but only allow limited data submissions per day [30]. Thus, we need an advanced data reduction algorithm to reduce submitted data to the cloud, reduce computing complexity, and increase battery life.

To operate ECG signals with low power and lower execution time, it is imperative to implement a QRS detection algorithm that is computationally efficient. Several new algorithms [31], [32] have been proposed over the last few decades to detect QRS complexes. According to [32], there are various kinds of filters that researchers have used, including derivatives, digital filters, and filter banks. However, the success of these algorithms depends not so much on their computational complexity as on their performance. Therefore, IoT systems are not ideal for these methods.

The proposed system enables ECG signals to be continuously monitored in a non-contact manner from the SOF, one-hand palm & one-foot sole (1H1F), and the POH in addition to the reduction of data submission with full recovery in the cloud, reducing complexity and extending battery life.

III. System Design and Description

Figure 1 shows the components of the proposed system. It has ECG front end, embedded software module and on the right side its cloud service. Three electrodes, such as the +ve electrode, -ve electrode, and right leg drive electrode (RLD) sense both the electro potential changes caused by cardiac electrical activity. ADS1292r is used to capture the ECG signal as an electric signal. Data is then received from the module via the serial peripheral interface (SPI), and is then transmitted to cloud after applying edge computing to reduce redundant samples at the device's node.

A. Electrode Material

ECG measurements have been performed using a flexible electrode SFCF having a smaller size, lighter weight, bendability, and stretchability, and it causes no skin aversions, which

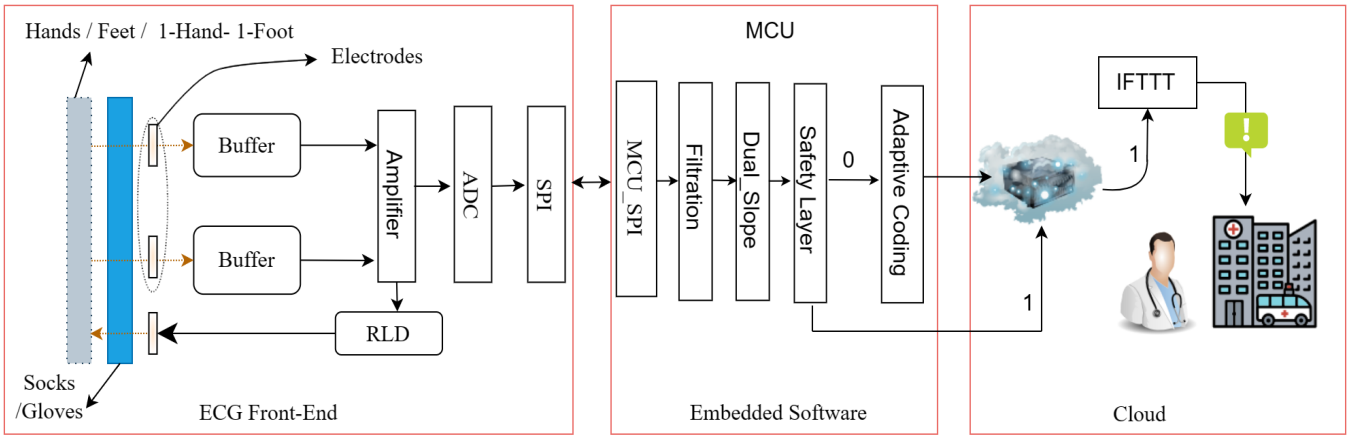

Figure 1. Architecture of the proposed system

makes it considered very user-friendly. Vacuum sputtering technology (VST) permanently bounds a small layer of uncontaminated silver to the flexible electrode's primary material SFCF. A silver percentage of between 15 and 18 percent is maintained for all electrode materials. Anti-oxidation is applied to the conductive fabric surface to make it resistant to washing. The silver is subsequently less prone to oxidation. A detailed description of the electrode can be found in Table I. Our systems consist of only 03 electrodes, such as the +ve electrode, -ve electrode, and RLD. This electrode set is flexible and stretchable, and will not irritate the subject.

Table I
DETAILED FEATURES AND CHARACTERISTICS OF ELECTRODE (SFCF)

Characteristics	Value
Thickness:	0.5 mm
Resistivity:	2- $Ohm.cm$
Weight:	0.12 $kg/m2$
Percentage of Silver:	15-18%
Temperature Range:	-30-85 degree centigrade
Other characteristics:	Flexible, stretchable, washable

B. Electrodes Placement

Human bodies are not static, especially in standing positions, and feet are far from the heart. It is also a challenge to measure ECG signals from feet sole due to their rougher skin than the chest or hands. Electrodes in this proposed system are designed like strips and placed horizontally when collecting ECG from feet as shown in Fig.2b. Foot contact can be maintained with electrodes even after slight movement. In the case of ECG collection from hands, electrodes are placed on a table as shown in Fig.2c. In the case of one hand and one foot (1H1F), one electrode is placed on the table while the other 2 electrodes are placed under the feet including RLD as shown in Fig.2d.

Electrode areas with larger spaces receive more electromagnetic radiation from the surrounding area. Therefore, electrodes with a large electrode area receive a lot of interference from electromagnetic waves. This problem is addressed by

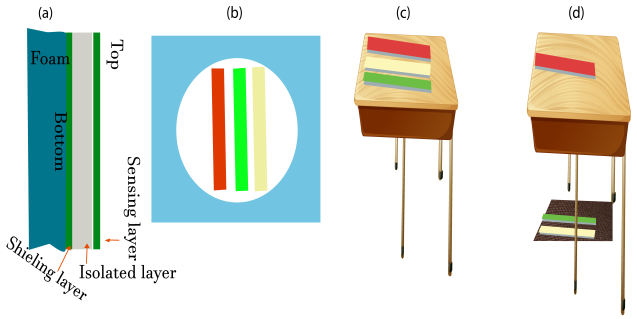

Figure 2. a) Active electrode structure; (b) Electrodes placement for feet (c) Electrodes placement for hands and (d) Electrode placement for one hand and one foot (1H1F)

placing an electromagnetic shield layer composed of SFCF underneath the active electrode, and by connecting the shield layer to the two electrodes with conductive fabric so that the potential of both shield layers is equal. As the conductive fabric is only about 0.5 mm thick, despite an increase in the shielding layer, the electrode remains thin. Fig.2a shows a schematic diagram of the active electrode.

The prototype to collect ECG from feet is shown in Fig.2b. In this arrangement, three electrodes are placed: the positive electrode is placed under the left foot, the negative electrode is placed under the right foot, and the RLD is approximately placed at the side of the right foot. A horizontal distance of about 5 cm exists between the two active electrodes. It is important to adjust this distance slightly, as different subjects have different-sized feet. Subjects wore socks to prevent their feet from getting dirty and to protect their bodies from accidental injury. In case the electrode needs to be cleaned after every use, we can do so, since it is washable.

A similar arrangement is also made in order to collect ECG from hands. In this arrangement, three electrodes are placed: the positive electrode is placed under the left-hand palm, the negative electrode is placed under the right-hand plam, and the RLD is approximately placed at the side of the right-hand

palm as shown in Fig.2c. However, in the case of 1H1F, the positive electrode is placed under the left-hand palm while RLD and negative electrodes are placed under the right foot sole as shown in Fig.2d.

C. Hardware Design

Since clothing separates the electrode from the skin, the impedance between the electrode and skin is much higher when ECG readings are taken through clothes. Additionally, the difference between electrode potentials is very small and leads to interference. It is possible to enhance the load capability and interference immunity of a circuit by incorporating an anti-interference buffer circuit. The schematic for the buffer circuit is shown in Fig. 3. It is equipped with an operational amplifier (OAP). In this study, a voltage follower with a gain of one is designed using an integrated circuit (IC) called AD8608 as the OAP. Hardware prototypes of the proposed system include the signals acquisition unit and data transfer unit.

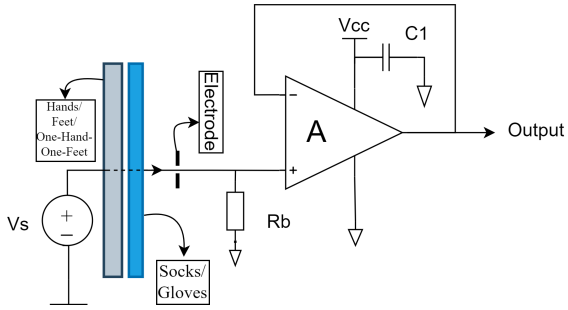

Figure 3. A schematic representation of the buffer circuit

The positive input end of the ECG acquisition channel is connected to a signal-sensing electrode placed under the left foot when collecting ECG from SOF. The negative input end is connected to another signal-sensing electrode shown in the ECG front end of Fig. 1. Moreover, the RLD circuit improves the quality of the ECG signal as well. Through the RLD electrode, it can transmit the common mode signal of two signal-sensing electrodes back to the user's body, thus improving the common mode rejection ratio (CMRR) of the ECG acquisition. In addition to the analog front end ADS1292, a programmable gain amplifier (PGA), an analog-digital converter (ADC), and an RLD circuit are implemented on the board.

Following the acquisition, data transmission modules receive ECG signals via SPI. The MCU and Wi-Fi module of the data transmission module transmits signals via Wi-Fi to the user interface, while the Xiaomi power bank supplies power to the hardware system. A prototype of the hardware for data collection is shown in Fig. 4. To transmit HR to the cloud, the ESP32's built-in WiFi module is used.

IV. Algorithms

A. Dual-Slope QRS Detection Algorithm

ECG signals are difficult to record from the SOF and POH when wearing socks and gloves because all types of noise

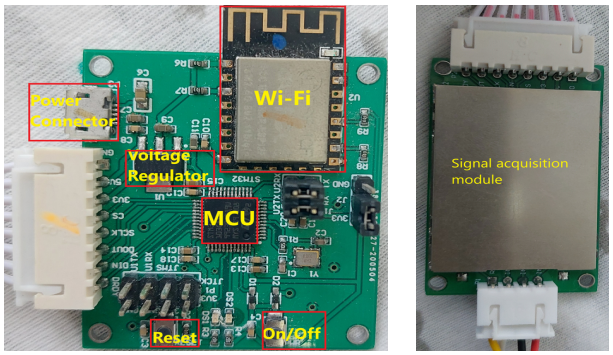

(a) (b)

Figure 4. A prototype of the hardware (a) Data transmission unit (b) Signal acquisition unit

are present. This includes baseline wander and interference from power lines, electromyography (EMG), and electrode motion artifacts. The raw ECG signal obtained from the SOF is depicted in Fig. 5.

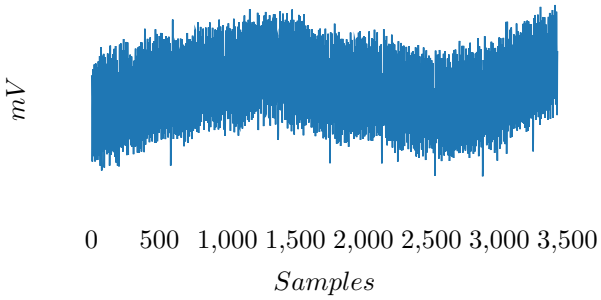

Figure 5. Raw ECG signal from SOF with socks

A baseline wander is a low-frequency noise that ranges between 0.5 Hz and 0.6 Hz. To remove it, a high-pass filter of 0.5 Hz to 0.6 Hz can be applied. A notch filter set to 50 Hz or 60 Hz can be used to eliminate power line interference. By using a low-pass filter with an adequate cutoff frequency (in our case, 40 Hz), we can filter out the EMG noise above 100 Hz. Motion artifacts can be reduced by minimizing the movement of the subject.

In our non-contact ECG system, enlarged electrodes proved to be a factor for power interference because electrodes were positioned closer to the ground. A number of double peaks were detected, and in some instances, the original peaks could not be detected due to baseline wanders and motion artifacts. To address this issue, we have implemented a high pass, low pass, and a notch filter. After removing all these distortions, we have implemented a dual slope algorithm to detect peaks [33].

An ECG signal usually includes three peaks Q, R, and S, which denote a single event occurring on a periodic basis. The Q wave deflects downward in the cycle, followed by the R wave's steepest upward deflection, and then the S wave's downward deflection. During this event, the time remains relatively constant, running between 0.06 second (sec) and 0.1 sec [34]. In the ECG signal, the slope at the R point should be large, the width should be narrow and the height

must be high. This prompted a small group of researchers to propose a dual-slope QRS detection method, which has minimal computing requirements and higher accuracy [33], [35]. The algorithm also has low hardware requirements. However, it must perform complicated slope calculations on both sides of each sample, which takes time. By focusing on one sample between 0.03 sec and 0.05 sec, we can calculate the slope from both sides, instead of highlighting all sample points. In QRS complexes, multiplying both slopes rather than taking the difference over the R peak produces higher values at the R peak. To get a high slope at R peaks, it is important to highlight a sample on both sides of the current sample. Only one sample 0.03 sec away from the current sample was used to calculate the slopes.

1) Filtering Method: The use of filters helps identify real peaks in ECG signals by filtering out the noise. Fig. 6 shows a filtered ECG signal after the implementation of these filters. A cutoff frequency of f_c 0.5 Hz is used for the high pass filter and a f_c of 40 Hz for the low pass filter. Before moving on to the next step, we need to eliminate power noise and baseline wanders. Otherwise, the peak count will differ from the real peak count.

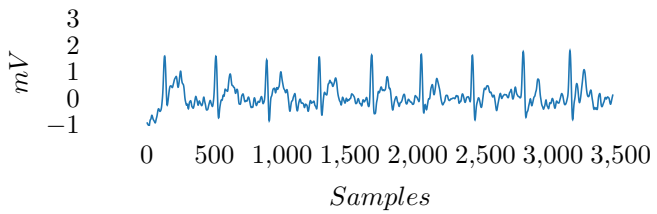

Figure 6. Filtered ECG signal from SOF with Socks

2) Slope Calculation: Slopes are calculated using equations (1) and (2).

$$Slope_{(Left)} = \left(\frac{E_i - E_{(i-k)}}{k}\right) \tag{1}$$

$$Slope_{(Right)} = \left(\frac{E_i - E_{(i+k)}}{-k}\right) \tag{2}$$

where E_i represents the current sample while $E_{(i-k)}$ and $E_{(i+k)}$ represent the two data samples on both sides of the current sample that are $0.03 \times f_s$ away from the current sample. f_s denotes sampling frequency where k is equal to the closest integer value of $0.03 \times f_s$. A steepness measurement parameter $Slope_{Multi}$ is determined as follows:

$$Slope_{Multi} = Slope_{(Left)} \times Slope_{(Right)} \tag{3}$$

The following requirement is verified when assessing the R peaks.

$$sgn(Slope_{(Left)}) = -sgn(Slope_{(Right)}) \tag{4}$$

To avoid inaccurate beat detection, the $Slope_{Multi}$ needs to be higher compared to a threshold value. To define a universal adaptive threshold technique based on the first three sec of data, a learning stage is introduced which requires at least two QRS complexes in order to initialize parameters according to the RR-interval. As a result, $Slope_{Multi}$ has been calculated for the first three sec in order to initialize the detection threshold and RR-interval-dependent parameters. Next, the detection threshold is determined as follows:

$$T = \left(\frac{Max(Slope_{Multi})}{3}\right) \tag{5}$$

Basically, it means that an ECG signal is classified as an R peak if the value of $Slope_{Multi}$ for the first three sec is greater than 1/3 of the maximum value of $Slope_{Multi}$ for that particular cycle. As a result of the ECG changing after every 8 detected peaks, the threshold for future signal sections was updated based on the average value of $Slope_{Multi}$ using the following equation:

$$T = avg(Slope_{Multiavg}) \tag{6}$$

where $Slope_{Multi_{avg}}$ denotes the mean of recent eight recorded peaks of the $Slope_{Multi}$.

3) Interval Window Between Two R Peaks: The interval between R-R peaks for a healthy individual heart is between 0.6 sec - 1 sec. However, R peaks sometimes appear more rapidly than the average in reaction to increased anxiety. Physiologically, however, there is a 200-millisecond refractory period that must elapse before the next R peak can emerge [36]. Using the most recent RR interval values, a "moving window" of time can be used to detect QRS complexes faster. It can be calculated as follows to ensure reliability:

$$RR_{int} \pm \Delta R \tag{7}$$

In this case, RR_{int} is the average interval between the last eight recorded peaks, and ΔR is $0.48 \times f_s$. To minimize the incidence of false negatives, this ΔR is meticulously chosen based on the refractory time and average RR-interval of human hearts.

During this time period, there should only be one peak seen for a resting heart. As described previously, it is likely that R peaks will recur more frequently than the average. Additionally, T waves, P waves, or noise sections are also capable of generating large slopes. In comparison to QRS complexes, these slopes are generally considerably smaller. A comparison is carried out between two peaks within a single window period in order to avoid incorrectly detecting R peaks if they occur within the same window period. As long as both of them are larger than a certain threshold, they are considered R peaks. Conversely, the peak with the highest value of $Slope_{Multi}$ only counts as an R peak. The condition is as follows:

$$H_{cur} > H_{ave} \times \alpha \tag{8}$$

Due to the fact that ECG signals are collected from different parts of the body, α varies based on the location; For hands, both standard devices and the proposed device without gloves the value of α was set to 0.7. However, when with gloves, the value of α was 0.5. In the case of sitting and standing positions, $\alpha = 0.3$ and 0.2, respectively.

4) Search for Local Extremes and Adjustments: Hands, chest and feet present different amplitudes of ECG voltage signals. Furthermore, switching between patients' ECGs can reduce the R peak signal and the ECG voltage amplitude. Low slopes may make it impossible to detect peaks in that region using a threshold calculated by comparing previously detected peaks. An algorithm like this should be easily adaptable without requiring intensive training. As a consequence, if an interval equivalent to the average QRS period has passed by without a cardiac rhythm being recorded, the threshold is halved by the previous threshold. By searching back through the same time interval, sensitivity can be increased to avoid missing actual R peaks in that region.

5) Adjustment within QRS Complex: When all the aforementioned conditions are met, the subsequent QRS complex maxima and minima will be evaluated in the current signal segment. This will enable us to locate the position of R peaks. During the analysis, the peak with the highest $Slope_{multi}$ value is kept as an R peak, while the others are discarded. Fig. 7, shows peak detection using a dual slope algorithm for SOF data.

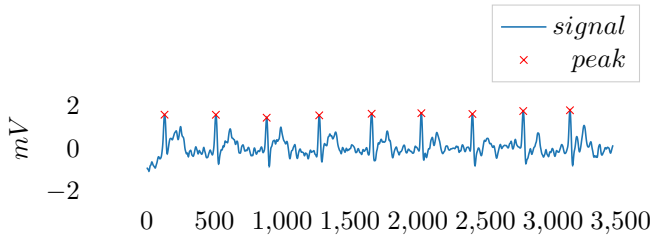

Figure 7. Peaks detection: ECG signal from SOF with socks

B. Adaptive Coding Algorithm

Many health-related applications are deployed on cloud-based platforms because of the ease of integration, the possibility to have advanced analytics, and the user-interface capabilities they offer. All this needs real-time data transmission which is not always a viable option because many health devices are battery-powered systems limiting the possibility to send data in real-time to the cloud. Therefore, we propose an adaptive algorithm that reduces the amount of data transmitted to the cloud without losing any essential information. The proposed algorithm divides data into samples that repeat and those that do not repeat. Redundant data sample values (repeating ones) are discarded and only their indexes are used to make data packets as illustrated in Fig. 8. In the cloud, these data packets are decomposed into samples based on their structure. Furthermore, energy efficiency is increased.

1) Proposed Algorithm: As part of our previous research [6], we implemented a data reduction algorithm for the purpose of removing redundant environmental data; however, environmental data differs greatly from the ECG data because the variability of ECG data is much greater over a short period of time than that of environmental data. Therefore, the earlier algorithm performs weakly with the ECG data. The proposed adaptive coding algorithm on the other hand eliminates efficiently HR ECG samples and retains only the information needed to reconstruct the originating data in the cloud. The proposed algorithm does not lose information when removing redundant information and retaining the essential information needed to restore the source data. Fig. 8 illustrates the operation of the algorithm.

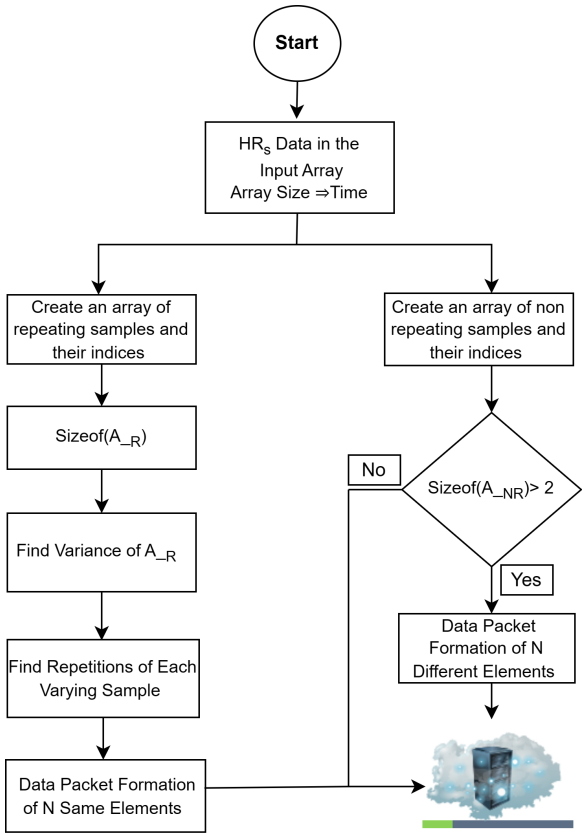

Figure 8. Adaptive coding to reduce cloud submissions

2) Operation of Adaptive Coding Algorithm: An input array is used to store HR data before the adaptive coding algorithm is executed. Sensor node resources and recording time of HR samples determine the length of the array. Prior to executing our algorithm, we store the first two minutes of samples.

After storing the samples in the input array. The next step is to separate the input array into redundant (the left branch) and non-redundant (right branch) arrays denoted as A_R and A_{NR}, respectively.

Then is calculated the array size of A_R and variance V of A_R. Variance is defined as how many different elements are stored in A_R. In addition, we also calculate how many times an element is repeating itself.

After calculating the variance V and the size of A_R, we calculate the repetition of each element R_E. To reduce the length of each data packet, we need to further split it into smaller data packets. Splitting a data packet depends on a split ratio S_r that is optimized to minimize the number of submissions to the cloud. By selecting S_r=5, we can reduce at a maximum 80% of the data we are supposed to submit to the cloud, while by selecting S_r=10, we can reduce at a maximum

90%. However, the selection depends on V and R_E. So, in general, having V =5 does provide enough performance for the data reduction process based on experimental analysis and it keeps the length of packets appropriate. In the case of A_{NR}, however, we first check the size of it, and if it is smaller than three, we send the sample directly to the cloud. Otherwise, a data packet formation is executed before sending it to the cloud.

Cloud Service and Emergency Response: We have used the same cloud service and emergency response system as explained in our previous study [6] and illustration is given in Fig. 9.

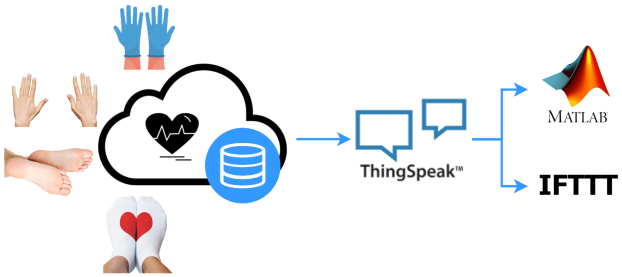

Figure 9. The ECG data were analysed in MATLAB along with IFTTT to respond to HR changes.

V. Results

A. Experiment Setup

Fig.10a illustrates the various devices and modules that are used in real-time for data collection. In addition, it demonstrates three figures as Fig.10b, Fig.10c, and Fig.10d for data collection with a mask, with socks in a sitting position, and with gloves. Fig.11 provides a complete illustration of data collection including electrode placement and connections for the standard device (PSG) and proposed device.

B. Validation of a Proposed System for ECG Signals Using a PSG Device as a Reference Standard

To properly validate the results of the proposed monitoring system, it is crucial to compare its outcomes with a reliable reference signal. Thus, the experiment employed a PSG system (Grael, Compumedics, Victoria, Australia) to concurrently capture ECG signals. The PSG device is typically equipped with multiple sensors that are attached to the patient's body to measure various physiological signals such as electroencephalography (EEG), electrooculography (EOG), electromyography (EMG), and ECG. Furthermore, the PSG system complies with all medical and manufacturing regulatory requirements, including the FDA (Food and Drug Administration) of the USA, ISO 13485 Quality Systems-Medical Devices, CE Mark (Europe), and many more [37].

A PSG device consistently produces high-quality recordings of ECG signals during rest. It is specifically engineered to diminish interference from other physiological factors like respiratory motion and muscle activity, which could potentially degrade ECG signal quality. In addition, the PSG device

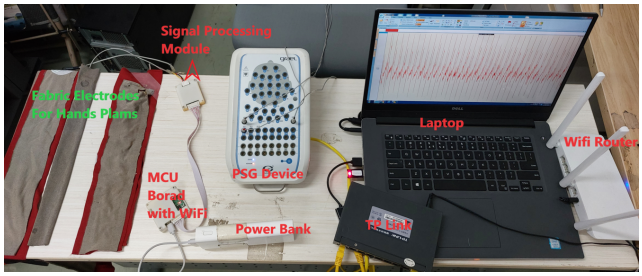

(a)

(b)

(c)

(d)

Figure 10. Experimental setup

adheres to a standardized methodology for capturing and scrutinizing ECG signals. This guarantees consistent and reliable data across a multitude of studies [38]–[40].

Typically, in PSG devices, ECG signals are acquired using silver/silver chloride (Ag/AgCl) electrodes in a single-lead configuration, and the same protocol was followed in our experiment.

In Fig.11, electrode positioning is shown for both the proposed and PSG systems. Wet electrode electrodes were utilized in the PSG system and are affixed to the subjects' wrists as shown in Fig.11. This arrangement facilitates precise and concurrent capture of ECG signals, enabling appropriate comparison of data gathered from the proposed monitoring system. Through the analysis of these signals, the new system's efficacy and dependability can be evaluated and confirmed.

C. Securing Informed Consent and Collecting Participant Details

Prior to commencing the collection of ECG data, we obtained informed consent from all participants, ensuring that the study's objectives were clearly explained. For child participants, consent was obtained from their parents. To obtain comprehensive information, we collected vital data, such as participants' names, ages, genders, heights, smoking habits, and any supplementary health or medical condition details.

The duration of data collection varied depending on the age group of participants. Adult and elderly participants underwent 50 minutes of data collection, which involved 10 minutes of data acquisition with and without a mask. On the other hand, we conducted data collection for children in shorter segments of 2 to 5 minutes each, accumulating a total duration of 22 to 30 minutes per child.

D. Illustration of Data Collection

A non-contact IoT-based measurement system is set up for capturing the ECG signal. An electrode that is flexible, lighter,

bendable, stretchable, and does not cause skin irritation is used to acquire ECG signals. In order to verify that the proposed system is useful, especially for the elderly, and keeping their needs in mind, we designed an experiment in such a way that standard device electrodes are connected with hand wrists while POH or SOF are positioned on fabric electrodes as shown in Fig.2.

Data collection prototypes in various positions are presented in Fig.11 and there are three electrodes connected to the PSG device: red, black, and green. Red signifies positive, black signifies negative, and green signifies RLD. However, in the proposed device, red indicates positive, green indicates negative and yellow indicates RLD. Fig.11a and Fig.11b represent data collection without and with mask respectively. The subject sits on a chair with electrodes attached to their wrists.

In our study, we have used two devices to compare ECG waveforms as shown in Fig.10a and Fig.11. The PSG and its electrodes are always attached to the wrists as pictured in Fig.11. The electrodes of SFCF, however, are positioned under the soles of the feet while socks are worn in standing and sitting positions. For the proposed device, the positive electrode is positioned under the left foot, the negative electrode is positioned at the right foot, and the RLD electrode is positioned at the side of the right foot as shown in Fig.11c and Fig.11d. However, in the case of 1H1F as shown in Fig.11e, 02 electrodes negative and RLD are positioned under the right foot sole while the positive electrode is positioned under the left-hand palm. When collecting ECG signals from hands, the positive electrode is positioned under the left-hand palm, and the negative electrode as well as the RLD electrode is positioned under the right-hand palm, as shown in Fig.11f. By simultaneously collecting the ECG signals with the reference device and proposed device helped us to compare the positions of QRS complexes.

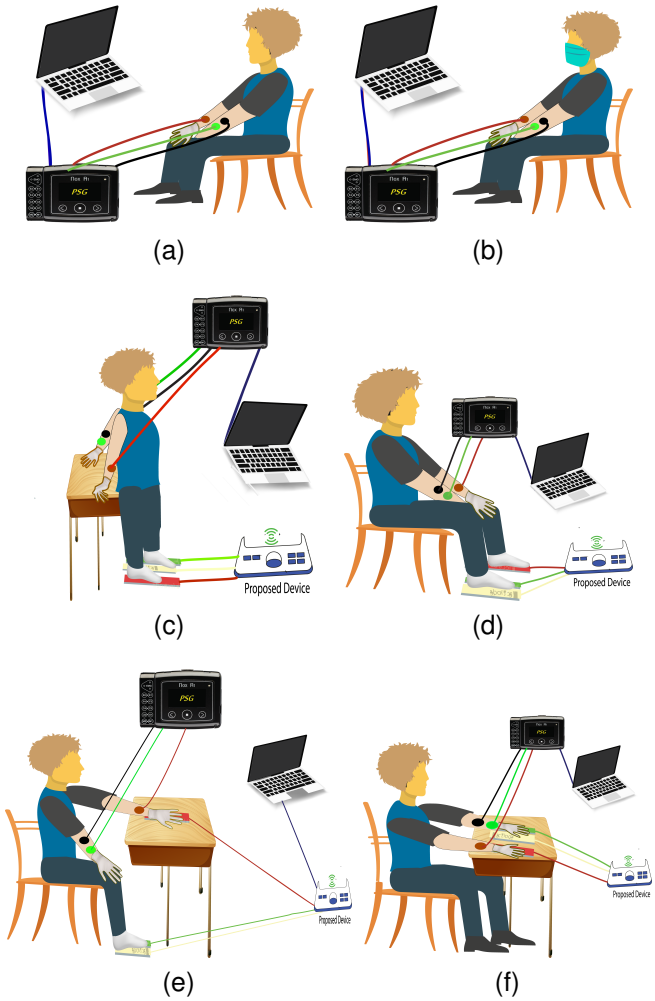

Figure 11. (a) Without mask (b) With mask (c) Standing with socks (d) Sitting with socks (e) 1H1F with a sock and a glove (f) With gloves

E. Data Collection Steps

The data collection steps (DCS) involved eight steps, and for adults, we calculated five minutes of data per step; for children, the time was reduced to around two minutes per step. We also collected ECG data while wearing a mask and without one to investigate whether the mask affects heartbeats. A consent form was completed as mentioned in section V-C. During the experiment, some observations were made that affected ECG data collection discussed in section VI. A total of 35 subjects participated in the study, including children, adults, middle-aged adults, and elderly individuals. Below are the steps for data collection.

1) From the POH without gloves (DCS1)
2) From the POH with gloves (DCS2).
3) From one hand palm, and from one-foot sole without a sock and glove (DCS3).
4) From one hand palm, and from one-foot sole with a sock and a glove (DCS4).
5) From the SOF without socks in a sitting position (DCS5).
6) From the SOF with socks in sitting position (DCS6).
7) From the SOF without socks in standing position (DCS7).
8) From the SOF with socks in standing position (DCS8).

F. Hands Palm

ECG from hands plam arrangement is shown in Fig.11f with gloves. Both hand palms are positioned on flexible electrode SFCF as well as reference portion of SFCF is also positioned under the right-hand palm. However, for standard devices, the positive electrode is attached to the left-hand wrist while the negative electrode as well as the reference electrode is attached to the right-hand wrist. During measurements, the volunteer's hand palms are tested with and without gloves on, in which case the ECG signal is obtained in contacting way as well as a non-contacting way. Fig.12a and Fig.13a illustrate the ECG signal from the PSG device, while Fig.12b and Fig.13b show the ECG signal without gloves and with gloves, respectively, using the proposed device.

G. 1H1F

ECG from 1H1F arrangement is shown in Fig.11e with a sock and glove on. In 1H1F ECG capturing arrangement is

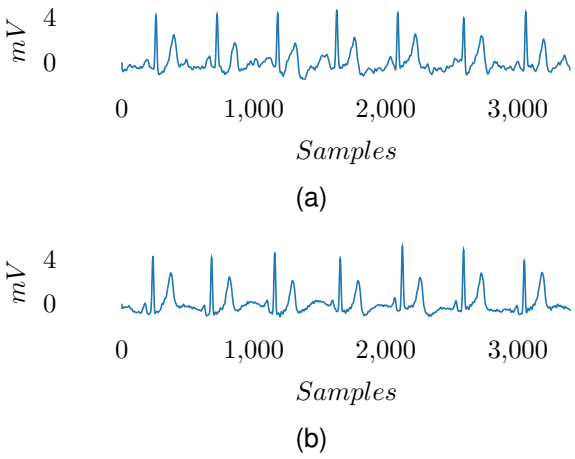

Figure 12. (a) An ECG taken with a PSG device from the wrists of the hands (b) Proposed device: ECG from hands palms without gloves

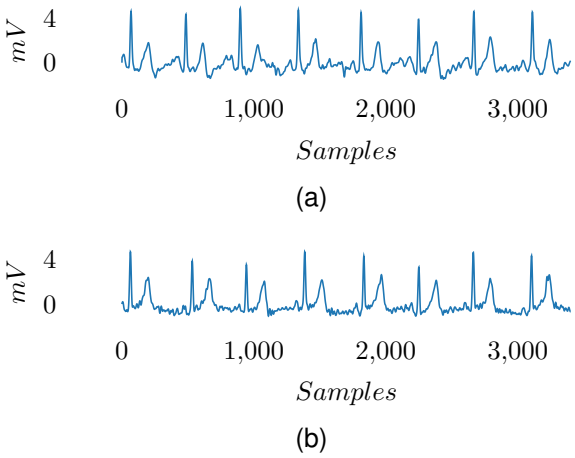

Figure 13. (a) An ECG taken with a PSG device from the wrists of the hands (b) Proposed device: ECG from Hands palms with Gloves

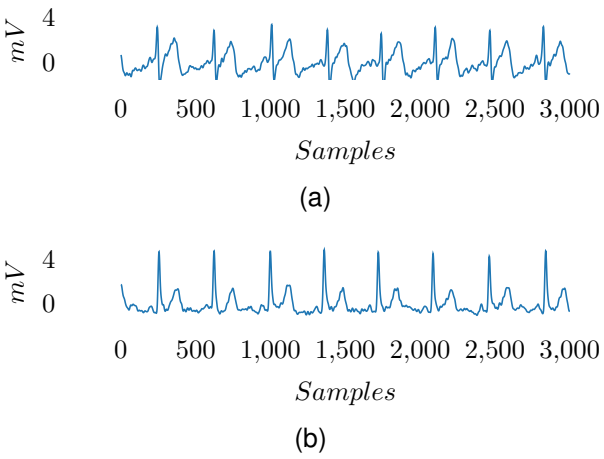

Figure 14. (a) An ECG taken with a PSG device from the wrists of the hands (b) Proposed device: ECG from 1H1F without a sock and glove

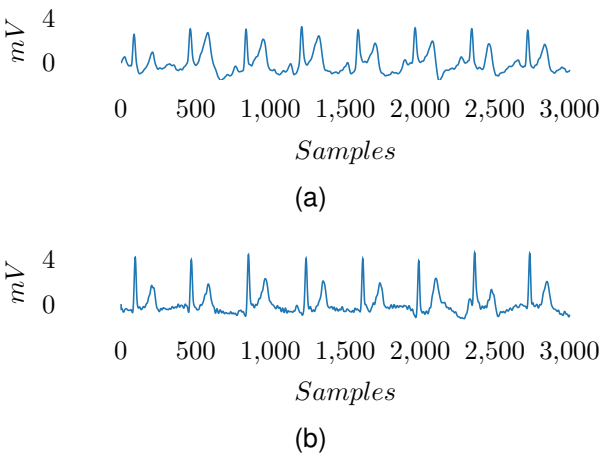

Figure 15. (a) An ECG taken with a PSG device from the wrists of the hands (b) Proposed device: ECG from 1H1F with a sock and glove

such as the negative electrode of SFCF is positioned under the right foot and the positive electrode under the left-hand palm while the RLD electrode is positioned under the right-foot heel to reduce common mode interference. For the PSG device, the electrode connection is the same as explained in section V-F.

During measurements, the volunteer's foot and hand are tested with and without a sock and glove on, in which case the ECG signal is obtained in contacting way as well as a non-contacting way. Fig.14a and Fig.15a show ECG signals from the wrists using the PSG device. Fig.14b and Fig.15b depict ECG signals from 1H1F without a sock on the right foot and a glove on the left hand, and with a sock on the right foot and a glove on the left hand, respectively.

H. ECG Signal from SOF

1) Standing: ECG from SOF in a standing position is shown in Fig.11c. In standing ECG capturing arrangement is such as negative electrode of SFCF is positioned under the right foot and positive electrode under the left foot sole while RLD electrode is positioned under the right foot heel to reduce common mode interference. For the PSG device, the electrode connection is the same as explained in section V-F. During measurements, the volunteer's feet are tested with and without socks on, in which case the ECG signal is obtained in contacting way as well as a non-contacting way. Fig.16a and Fig.17a display ECG signals from the wrists captured using the PSG device. Fig.16b and Fig.16b demonstrate the ECG signal in a standing position, without socks and with socks, respectively.

2) Sitting: SFCF electrode placement for ECG collection from SOF while sitting is the same as standing. Fig.18a and Fig.19a display ECG signals from the wrists captured using the PSG device. Fig.18b and Fig.19b demonstrate the ECG signal in the sitting position, without socks and with socks, respectively.

I. Analysis of HR and RR Interval Measurements from Proposed ECG Device Compared to PSG Device

HR and RR intervals are important parameters in analyzing ECG signals for assessing cardiovascular health. HR, measured as bpm, is calculated by measuring the time between two consecutive R peaks in an ECG signal. RR interval, which is the duration between successive R peaks, is an indicator of

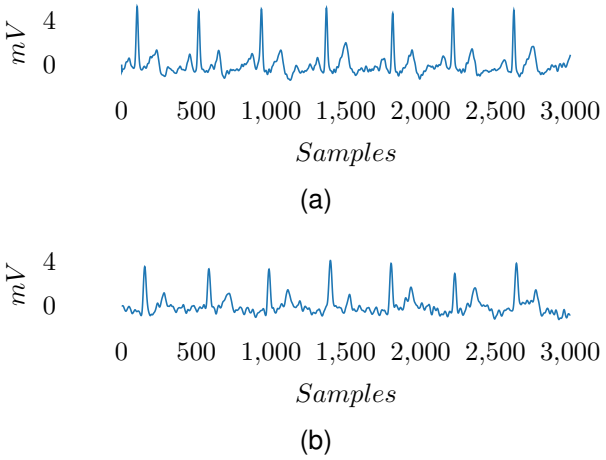

Figure 16. (a) An ECG taken with a PSG device from the wrists of the hands (b) Proposed device: ECG from SOF in Standing Position Without Socks

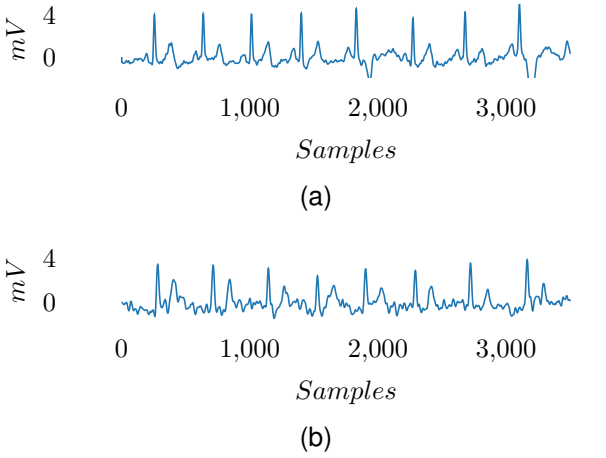

Figure 17. (a) An ECG taken with a PSG device from the wrists of the hands (b) Proposed device: ECG from SOF in Standing Position with Socks on

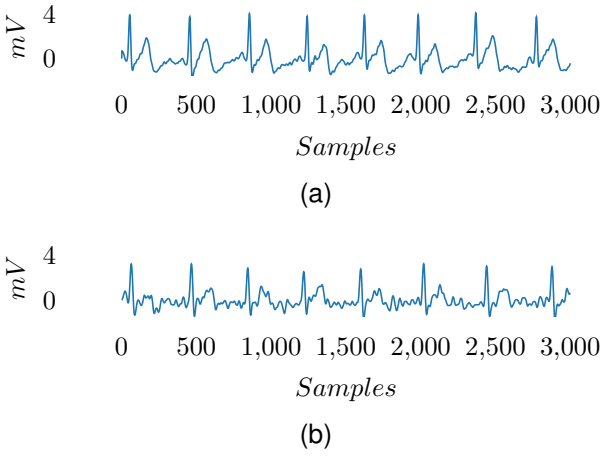

Figure 18. (a) An ECG taken with a PSG device from the wrists of the hands (b) Proposed Device: ECG from SOF in sitting position without socks

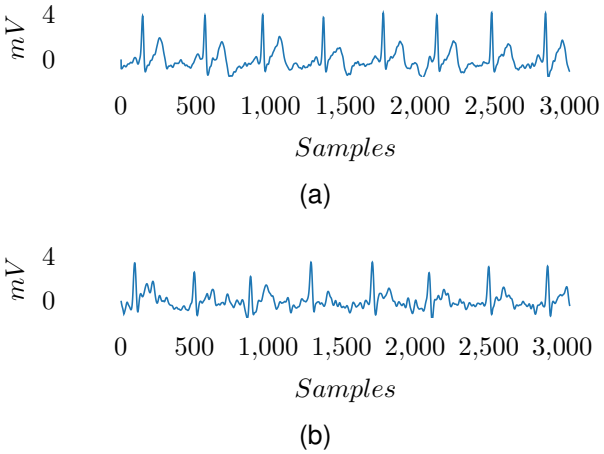

Figure 19. (a) An ECG taken with a PSG device from the wrists of the hands (b) Proposed device: ECG from SOF in a sitting position with socks

the heart's rhythm regularity and can reveal irregularities like arrhythmia.

Comparing HR and RR interval measurements from the proposed ECG device with those from a standard PSG device can help determine the accuracy and reliability of the proposed device. PSG monitors multiple physiological parameters, including ECG, to provide a comprehensive picture of a patient's health. The strong correlation between measurements from the proposed ECG device and the PSG device would indicate the accuracy and reliability of the device for monitoring HR and RR intervals.

Gathering ECG data for varying time periods can influence the accuracy and precision of measurements derived. The optimal duration for collecting ECG data is contingent upon the particular application or setting in which the information is being obtained.

The provided tables, namely Table II, Table III, and Table IV contain data for the average HR and the average HR estimation error of the proposed device compare to a PSG device. The purpose of these tables is to facilitate a comparative analysis between the two devices.

Table II
COMPARISON OF 2-MINTUES AVERAGE HR (BPM) BETWEEN PROPOSED DEVICE AND PSG AND AVERAGE HEART RATE ESTIMATION ERROR

	Subject-1 (S1): Adult		S2: Elderly		Avg-HR-Diff
DCS	Proposed	PSG	Proposed	PSG	S1 & S2
DCS1	69	69	77	76	0.5
DCS2	64	64	83	82	0.5
DCS3	69	69	81	81	0.0
DCS4	68	68	83	82	0.5
DCS5	69	68	82	81	1.0
DCS6	71	69	82	82	1.0
DCS7	72	72	84	85	0.5
DCS8	73	72	85	85	0.5

In Table II, the estimation errors for DCS5 and DCS6 were found to be the highest while collecting data from SOF while sitting on a chair with and without socks on. On the other hand, DCS3, which involved capturing ECG signals from 1H1F without a sock and glove on, had the lowest average

HR difference. For two minutes of average HR, the average estimation error was approximately 0.56 BPM for the subjects mentioned in the Table.

However, when comparing the average HR estimation error for 1 minute, as shown in Table III, it was found that DCS1 showed the least average HR estimation error of 0 while DCS6 showed the highest with an average HR estimation difference of 2 BPM, resulting in an overall estimation average of 0.75 BPM for Table III.

In Table IV, when comparing the average HR of 30 seconds, DCS1 showed the least average HR difference of 0.5 while DCS6 showed the highest with an average HR difference of 3. However, if we combine the average HR difference of all three tables and calculate the average HR estimation error, it is found to be 0.7916 BPM, indicating that the system is reliable for remote monitoring. After analyzing the data of all 35 subjects using the same meticulous process and calculating the average HR estimation for all participants, it was determined that the average HR estimation was approximately ∓ 1.

Table III
COMPARISON OF 1-MINUTE AVERAGE HR (BPM) BETWEEN PROPOSED DEVICE AND PSG AND AVERAGE HEART RATE ESTIMATION ERROR

	S1: Adult		S2: Elderly		Avg-HR-Diff
DCS	Proposed	PSG	Proposed	PSG	S1 & S2
DCS1	71	71	78	76	0.0
DCS2	64	64	83	82	0.5
DCS3	69	69	83	83	0.0
DCS4	70	70	83	83	0.0
DCS5	70	70	83	81	1.0
DCS6	72	69	82	83	2.0
DCS7	72	73	85	83	1.5
DCS8	73	73	86	84	1.0

Table IV
COMPARISON OF 30 SECONDS AVERAGE HR (BPM) BETWEEN PROPOSED DEVICE AND PSG AND AVERAGE HEART RATE ESTIMATION ERROR

	S1: Adult		S2: Elderly		Avg-HR-Diff
DCS	Proposed	PSG	Proposed	PSG	S1 & S2
DCS1	71	72	77	77	0.5
DCS2	62	63	80	81	1.0
DCS3	68	67	82	83	1.0
DCS4	68	68	83	84	0.5
DCS5	68	69	82	81	0.5
DCS6	71	67	82	80	3.0
DCS7	71	71	85	84	0.5
DCS8	73	71	86	85	1.5

Similarly, Table V, Table VI, and Table VII provide the average R-R intervals of an elderly and an adult participant over different time intervals (2 minutes, 1 minute, and 30 seconds). The data in these tables indicate that the proposed device and the standard PSG device have quite similar RR intervals except for an adult in Table VI DCS6 and Table Table VII DCS6 and DCS8. This is significant because it shows that the proposed device is a viable option for evaluating cardiovascular health by measuring heart rate variability and HR.

During data collection in steps 7 and 8 (SOF while standing), assistance was provided to the subjects to capture the ECG signal. Without assistance, the data collected from most subjects even after filtration was noisy. However, subjects with short height and low body fat were able to provide data without assistance. Nonetheless, all subjects were asked to have assistance while standing, as shown in Fig.11c.

Table V
COMPARISON OF 2-MINUTES MEAN R-R INTERVALS BETWEEN PROPOSED DEVICE AND PSG

	S1: Adult		S2: Elderly	
DCS	Proposed	PSG	Proposed	PSG
DCS1	0.8750	0.87340	0.7751	0.7898
DCS2	0.9349	0.9321	0.7226	0.7317
DCS3	0.8722	0.8685	0.7402	0.7377
DCS4	0.8776	0.8840	0.7194	0.7398
DCS5	0.8755	0.8800	0.7342	0.7362
DCS6	0.8444	0.8699	0.7347	0.7298
DCS7	0.8345	0.8316	0.7186	0.7050
DCS8	0.8165	0.8319	0.7112	0.7081

Table VI
COMPARISON OF 1-MINUTE MEAN R-R INTERVALS BETWEEN PROPOSED DEVICE AND PSG

	S1: Adult		S2: Elderly	
DCS	Proposed	PSG	Proposed	PSG
DCS1	0.8505	0.8494	0.7663	0.7876
DCS2	0.9414	0.9391	0.7231	0.7331
DCS3	0.8688	0.8699	0.7252	0.7230
DCS4	0.8526	0.8511	0.7243	0.7210
DCS5	0.8548	0.8529	0.7241	0.7410
DCS6	0.8371	0.8740	0.7299	0.7272
DCS7	0.8276	0.8246	0.7023	0.7234
DCS8	0.8225	0.8205	0.6990	0.7181

Table VII
COMPARISON OF 30 SECONDS MEAN R-R INTERVALS BETWEEN PROPOSED DEVICE AND PSG

	S1: Adult		S2: Elderly	
DCS	Proposed	PSG	Proposed	PSG
DCS1	0.8428	0.8368	0.7755	0.7746
DCS2	0.9617	0.9565	0.7513	0.7499
DCS3	0.8800	0.8990	0.7298	0.7258
DCS4	0.8790	0.8840	0.7212	0.7401
DCS5	0.8811	0.8711	0.7328	0.7401
DCS6	0.8445	0.8841	0.7314	0.7483
DCS7	0.8504	0.8393	0.7080	0.7140
DCS8	0.8165	0.8469	0.6993	0.7065

J. Adaptive Coding to Reduce Data Submission

In our previous study [6], a data reduction algorithm was developed to send minimal environmental sensor samples to the ThingSpeak cloud platform and store them in different fields. In this study, an adaptive coding algorithm is specifically designed for HR data, and its effectiveness is depicted in Fig. 20.

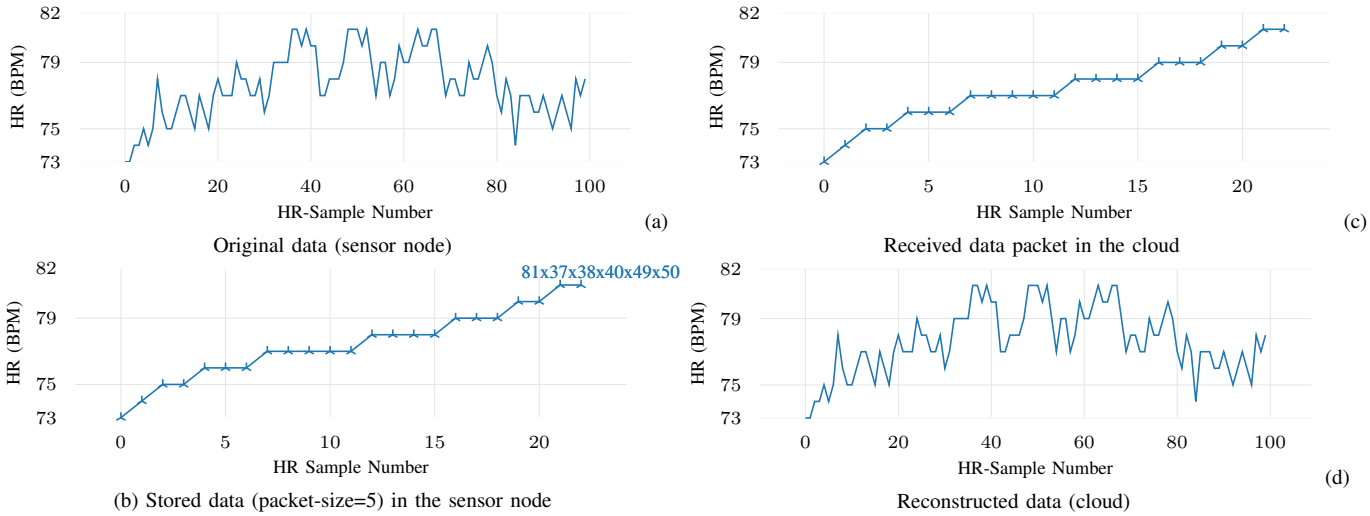

Figure 20. Implementation of adaptive coding to reduce and reconstruct samples

The original HR data samples are displayed in Fig.20(a), and are stored in the input array. After applying the adaptive coding algorithm in the sensor node, the subsequent Fig.20(b), shows the reduced data samples. The data is then converted into data packets in the form of a string, an example of which is shown in Fig.20(b). In this data packet, the value 81 represents HR, and all the values after "x" are the indexes on which it repeats itself. Therefore, when sending one data packet to the cloud, only the HR value of 81 is plotted in the packet.

Upon receiving the reduced data on the cloud side, as shown in Fig.20(c), we were able to reconstruct the original HR data samples, as demonstrated in Fig.20(d). This process enables efficient transmission of data from the sensor node to the cloud while providing full data reconstruction for analysis. In addition, it can also help to improve data security if it is applied with an encryption module as it can add one data security layer.

This process enables efficient data transmission from the sensor node to the cloud while providing full data reconstruction for analysis. Furthermore, implementing an encryption module with the proposed adaptive coding can bolster data security by adding an additional layer of protection.

K. HR Analysis in the cloud

We can download or analyze the complete data packets in the cloud. By leveraging the advanced data visualization and analysis tools provided by ThingSpeak, we can create, for example, interactive histograms that allow us to explore ECG data (HR) in more detail. An example histogram is shown in Fig.21, as they provide useful insights into the distribution of HR measurements in a dataset.

L. Different Age Groups Response to Face Masks

The wearing of facial masks for combating the Coronavirus disease outbreak is generally advised [41]. The purpose of this study was to examine the ECG and perceptual responses to

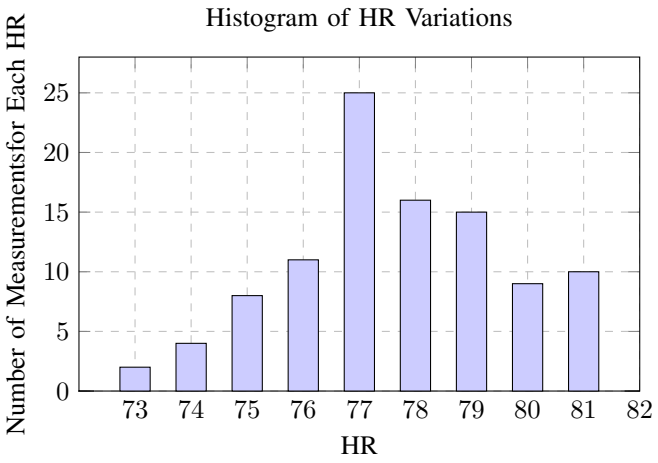

Figure 21. Histogram of Heart Rate Variations

medical face masks. In addition to helping to prevent COVID-19 spread, face masks have concerns about discomfort and impaired breathing, says Dr Shein, an Associate Professor of Pediatrics at Case Western Reserve University School of Medicine [42].

In [43], Dr Hall, carried out an investigation and measured her oxygen levels and HR whilst putting on various masks to prove that wearing masks did not hinder respiratory function. Her goal was to suggest the use of face masks as a preventive step against the disease COVID-19. Her experiments included no mask, a surgical mask, an N95 mask (a type of respirator), and an N95 plus surgical mask, which she says is what most US healthcare workers currently use. It turned out that all of her recordings were nearly identical. When she did not wear a mask, her oxygen saturation was 98 percent and her heart rate (HR) was 64 beats per minute (BPM). Her oxygen level remained stable while she wore the surgical mask, but her HR spiked to 68. Oxygen saturation was 99 percent and HR was 69 BPM with both N95 masks.

Our study examines how masks affect different age groups,

Table VIII
MASKS AND HR: FIVE MINUTE AVERAGE HR IN BPM FOR DIFFERENT AGE GROUPS

Age/Gender	Height	Weight	Without mask	With mask
34/M	180cm	85Kg	84.5	91.6
30/F	165cm	50Kg	60.5	64.3
30/M	185cm	73Kg	58.7	57.7
26/F	170cm	50Kg	86.7	87.2
56/M	178cm	80Kg	83.9	85.5
29/M	179cm	79Kg	74.9	80.3
34/M	165cm	67Kg	72.8	72.6
22/M	164cm	81Kg	84.8	84.9
22/M	167cm	60Kg	80.8	81.5
31/M	166cm	57Kg	94.3	96.8
26/F	163cm	46Kg	90.0	90.4
26/M	175cm	50Kg	80.0	81.9
28/M	172cm	63Kg	89.1	89.9
27/M	178cm	65Kg	72.6	73.0
59/M	181cm	92Kg	80.9	80.5
7/M	124cm	32Kg	81.1	78.5
8/M	134cm	26Kg	86.9	83.0
5/F	101cm	23Kg	97.3	83.0
8/M	128cm	25Kg	82.4	83.9
8/M	133cm	27Kg	101.3	99.0

including children, teenagers, adults, middle-aged people, and senior citizens. A total of 35 volunteers participated in the study. Fig.11a shows the subjects' first step in the experiment: they sat on a chair without masks for five minutes. The ECG was recorded using a PSG device. Next, participants were asked to wear masks and sit quietly while their ECG was recorded. The results are given in Table VIII.

Considering the results, it can be concluded that HR variation is different for different age groups. In the case of elderly people, HR changes were very slight. For example, for one elderly person, it increased from 83.9 to 85.5 BPM. For another, it barely changed at all. Adults, however, either have almost constant HR or it rises between one and six BPM. Contrary to the above two cases, children's HRs deviate from typical trends, declining with masks and increasing without. Children's average HR also showed the greatest variation, which was decremented by almost 14 BPM compared to while wearing a mask. It should be noted, however, that children were watching cartoons and serials while data was being collected.

VI. DISCUSSION

As far as we know, this is a first-of-its-kind IoT-based system that offers non-contact solutions to collect ECG which is especially useful for the elderly and other users benefiting from non-contact home measurement systems. In addition, the proposed system minimizes the submission of data samples to the cloud with the adaptive coding module. The adaptive coding enables full cloud-based reconstruction of the submitted samples.

Since electrodes can be positioned horizontally on a weight scale or on a table, the proposed system can potentially measure ECG signals at different positions. Therefore, we measured the ECG signals from the SOF with and without socks, and from POH with and without gloves as well as 1H1F with a sock and a glove. This needed us to adjust the constant α of the dual-slope algorithm to detect peaks with better accuracy, and thus reliably collect ECG through contact or without contact.

To collect ECG signals in a standing position in most tall and heavy subjects, assistance was required to balance the feet and reduce weight on electrodes. There was a slight difference in the angle between the knee and hip. It should be noted that the proposed system does not always allow for a clear ECG signal when standing. Therefore, we will undertake additional work in the future.

We were originally planning to collect data from 55 individuals including children, adults, and the elderly. However, due to COVID and the lockdown, we have only collected data from 35 individuals. In the future, when the COVID situation improves, we will carry out experiments on more subjects and more scenarios and investigate the impact of masks on the elderly, adults, and children.

VII. CONCLUSIONS

In this paper, we presented an IoT-Based Non-Contact ECG System design that can measure ECG signals with or without contact. The proposed system was tested with three different ECG measurement combinations: from the SOF with or without socks, from POH with or without gloves, or from 1H1F with or without a sock or a glove. In the tests, three electrodes were used, including two signal-sensing electrodes and one RLD electrode. The system is composed of three parts where the ECG front-end part includes flexible electrodes that are made from SFCF which are extremely comfortable and do not irritate the skin, the embedded part constitutes of a signal processing module, an adaptive coding algorithm that reduces data submission to the cloud, a WiFi module for transmission of data to the cloud part, and an interface that allows users to interact with the system. Ground truth data to validate our system was provided by the PSG system. The tests were carried out and 35 volunteers of various ages were recruited to participate in the experiment. The measurements demonstrate that the proposed system in comparison to the reference device can capture ECG signals with very low or no latency on the R peak. When evaluated with the ground truth signal, the extrapolated RR intervals signal has a very high correlation coefficient and a very small erroneous value.

REFERENCES

[1] World Health Organization (WHO). Disabled people in the world in 2021: Facts and figures. Accessed: 2022-02-10.

[2] United Nations. Department of economic and social affairs disability. Accessed: 2022-08-28.

[3] World Health Organization. Disability and health. March 2022.

[4] S Sankar, P Srinivasan, and R Saravanakumar. Internet of things based ambient assisted living for elderly people health monitoring. *Research Journal of Pharmacy and Technology*, 11(9):3900–3904, 2018.

[5] Goldman Sachs Report. How the internet of things can save the american healthcare system $305 billion annually. june 2016.

[6] Muhammad Irfan, Husnain Jawad, Barkoum Betra Felix, Saadullah Farooq Abbasi, Anum Nawaz, Saeed Akbarzadeh, Muhammad Awais, Lin Chen, Tomi Westerlund, and Wei Chen. Non-wearable iot-based smart ambient behavior observation system. *IEEE Sensors Journal*, 21(18):20857–20869, 2021.

[7] R. S. H. Istepanian, S. Hu, N. Y. Philip, and A. Sungoor. The potential of internet of m-health things "m-iot" for non-invasive glucose level sensing. In *2011 Annual International Conference of the IEEE Engineering in Medicine and Biology Society*, pages 5264–5266, 2011.

[8] Nilanjan Dey, Aboul Ella Hassanien, Chintan Bhatt, Amira S Ashour, and Suresh Chandra Satapathy. *Internet of things and big data analytics toward next-generation intelligence*. Springer, 2018.

[9] Melanie Swan. Sensor mania! the internet of things, wearable computing, objective metrics, and the quantified self 2.0. *Journal of Sensor and Actuator networks*, 1(3):217–253, 2012.

[10] Katie S Hahm and Brian W Anthony. In-home health monitoring using floor-based gait tracking. *Internet of Things*, page 100541, 2022.

[11] Nisha Kandhoul and Sanjay K Dhurandher. Deep q learning based secure routing approach for oppiot networks. *Internet of Things*, page 100597, 2022.

[12] Jarkko Hyysalo, Sandun Dasanayake, Jari Hannu, Christian Schuss, Mikko Rajanen, Teemu Leppänen, David Doermann, and Jaakko Sauvola. Smart mask–wearable iot solution for improved protection and personal health. *Internet of Things*, 18:100511, 2022.

[13] Naif Al Mudawi. Integration of iot and fog computing in healthcare based the smart intensive units. *IEEE Access*, 10:59906–59918, 2022.

[14] Raafat Aburukba, A. R. Al-Ali, Nourhan Kandil, and Diala AbuDamis. Configurable zigbee-based control system for people with multiple disabilities in smart homes. In *2016 International Conference on Industrial Informatics and Computer Systems (CIICS)*, pages 1–5, 2016.

[15] B. K. Hensel G. Demiris, B. K. Hensel. Technologies for an aging society: A systematic review of "smart home" applications: doi:10.1055/s-0038-1638580. Accessed: 2022-02-11.

[16] Max Grell, Can Dincer, Thao Le, Alberto Lauri, Estefania Nunez Bajo, Michael Kasimatis, Giandrin Barandun, Stefan A Maier, Anthony EG Cass, and Firat Güder. Autocatalytic metallization of fabrics using si ink, for biosensors, batteries and energy harvesting. *Advanced functional materials*, 29(1):1804798, 2019.

[17] Salome Oniani, GonÃ§alo Marques, Ivan Miguel Pires, Salome Muhkashavria, and Nuno M. Garcia. E-health and m-health applications in georgia: A review on the free available applications for android devices. In *2020 IEEE International Conference on Big Data (Big Data)*, pages 3793–3796, 2020.

[18] Anwar D. Alhejaili. M-health concept, services and issues. In *2021 1st International Conference on Artificial Intelligence and Data Analytics (CAIDA)*, pages 18–22, 2021.

[19] Ovidiu Vermesan and Peter Friess. *Internet of things: converging technologies for smart environments and integrated ecosystems*. River publishers, 2013.

[20] Emelia J Benjamin, Salim S Virani, Clifton W Callaway, Alanna M Chamberlain, Alexander R Chang, Susan Cheng, Stephanie E Chiuve, Mary Cushman, Francesca N Delling, Rajat Deo, et al. Heart disease and stroke statistics-2018 update: a report from the american heart association. *Circulation*, 137(12):e67–e492, 2018.

[21] Longrui Han, Xinyu Li, and Zewen Yang. The design of ecg preamplifier for wearable device. In *2021 3rd International Conference on Intelligent Control, Measurement and Signal Processing and Intelligent Oil Field (ICMSP)*, pages 226–229, 2021.

[22] Nipon Chattipakorn, Tanat Incharoen, Natnicha Kanlop, and Siriporn Chattipakorn. Heart rate variability in myocardial infarction and heart failure. *International journal of cardiology*, 120(3):289–296, 2007.

[23] Alhassan Haruna Umar, Mohd Afzan Othman, Fauzan Khairi Che Harun, and Yusmeeraz Yusof. Dielectrics for non-contact ecg bioelectrodes: A review. *IEEE Sensors Journal*, 21(17):18353–18367, 2021.

[24] Adam Bujnowski, Kamil Osinski, Artur Polinski, Tomasz Kocejko, Piotr Przystup, Diana Bogusz, and Jerzy Wtorek. Smart weighing scale with feet-sampled ecg. In *IECON 2018 - 44th Annual Conference of the IEEE Industrial Electronics Society*, pages 3286–3291, 2018.

[25] Birutė Paliakaitė, Saulius Daukantas, Andrius Sakalauskas, and Vaidotas Marozas. Estimation of pulse arrival time using impedance plethysmogram from body composition scales. In *2015 IEEE Sensors Applications Symposium (SAS)*, pages 1–4. IEEE, 2015.

[26] Joan Gomez-Clapers, Ramon Casanella, and Ramon Pallas-Areny. Pulse arrival time estimation from the impedance plethysmogram obtained with a handheld device. In *2011 Annual International Conference of the IEEE Engineering in Medicine and Biology Society*, pages 516–519. IEEE, 2011.

[27] Shun Peng, Ke Xu, Shenjie Bao, Yafei Yuan, Chenyun Dai, and Wei Chen. Flexible electrodes-based smart mattress for monitoring physiological signals of heart and autonomic nerves in a non-contact way. *IEEE Sensors Journal*, 21(1):6–15, 2021.

[28] Bin Yang, Yonggui Dong, Zhongjie Hou, and Xiaohui Xue. Simultaneously capturing electrocardiography and impedance plethysmogram signals from human feet by capacitive coupled electrode system. *IEEE Sensors Journal*, 17(17):5654–5662, 2017.

[29] Kara. Rogers. "what's the difference between bluetooth and wi-fi?". encyclopedia britannica. Feb 2022.

[30] Thingspeak prices. Feb 2022.

[31] Haoran Li. A novel dual-slope based electrocardiogram peak detection method for wearable devices. In *2020 IEEE 3rd International Conference on Information Systems and Computer Aided Education (ICISCAE)*, pages 327–331, 2020.

[32] M. Riadh Arefin, Kouhyar Tavakolian, and Reza Fazel-Rezai. Qrs complex detection in ecg signal for wearable devices. In *2015 37th Annual International Conference of the IEEE Engineering in Medicine and Biology Society (EMBC)*, pages 5940–5943, 2015.

[33] Y Wang, Chacko John Deepu, and Y Lian. A computationally efficient qrs detection algorithm for wearable ecg sensors. In *2011 Annual International Conference of the IEEE Engineering in Medicine and Biology Society*, pages 5641–5644. IEEE, 2011.

[34] Frank G. Yanowitz MD Professor of Medicine (Retired) University of Utah School of Medicin. Characteristics of the normal ecg. March 2022.

[35] Haoran Li. A novel dual-slope based electrocardiogram peak detection method for wearable devices. In *2020 IEEE 3rd International Conference on Information Systems and Computer Aided Education (ICISCAE)*, pages 327–331. IEEE, 2020.

[36] Jiapu Pan and Willis J Tompkins. A real-time qrs detection algorithm. *IEEE transactions on biomedical engineering*, (3):230–236, 1985.

[37] Compumedics Limited. Regulatory compliance. https://www.compumedics.com.au/en/aboutcompumedics/regulatory-compliance/, Accessed: 2023.

[38] Shun Peng, Ke Xu, Shenjie Bao, Yafei Yuan, Chenyun Dai, and Wei Chen. Flexible electrodes-based smart mattress for monitoring physiological signals of heart and autonomic nerves in a non-contact way. *IEEE Sensors Journal*, 21(1):6–15, 2021.

[39] Dean J Miller, Charli Sargent, and Gregory D Roach. A validation of six wearable devices for estimating sleep, heart rate and heart rate variability in healthy adults. *Sensors*, 22(16):6317, 2022.

[40] Piero Fontana, Neusa R Adão Martins, Martin Camenzind, René M Rossi, Florent Baty, Maximilian Boesch, Otto D Schoch, Martin H Brutsche, and Simon Annaheim. Clinical applicability of a textile 1-lead ecg device for overnight monitoring. *Sensors*, 19(11):2436, 2019.

[41] Eric Tsz-Chun Poon, Chen Zheng, and Stephen Heung-Sang Wong. Effect of wearing surgical face masks during exercise: Does intensity matter? *Frontiers in Physiology*, 12, 2021.

[42] University Hospitals Cleveland Medical Center. The impact of face masks on heart rate and oxygenation. Accessed: 2022-06-15.

[43] Jane Pearl. Covid-19: How does wearing mask affect heart rate and oxygen levels. Accessed: 2022-06-15.

VIII. Biography Section

Muhammad Irfan is a doctoral researcher since 2021 at Fudan University in Shanghai, China, and the University of Turku in Finland. He holds a master's degree in electronics and communication engineering from Fudan University (2021) and a bachelor's degree in electronics engineering from UET Taxila in Pakistan (2015). He received a scholarship grant from the Chinese government (CGS) for both his master's and PhD studies. He has practical experience as an assistant engineer and trainee engineer at AEDB and Pak Agro Tech in Islamabad, Pakistan (July 2015 - October 2016).In addition, he has also collaborated with Bear Net and Nile Intelligent Companies in Shanghai on 02 industrial projects. His research focuses on IoT, edge computing, intelligent sensor systems, and deep learning.

Shun Peng received doctor's degree in biomedical engineering in Fudan University, Shanghai, China, 2021. His research interests include non-invasive biomedical signal measurement, and the development of emerging technologies for biomedical signal processing and data analysis.

Barkoum Betra Felix is currently pursuing a master's degree with the faculty of engineering science at Paul Sabatier University, France. He is also affiliated with the Department of Measurement and Information Engineering at the University of Shanghai for Science and Technology, Shanghai, China. He graduated from the University of Shanghai for Science and Technology, Shanghai, China, in 2020 with a B.S. in telecommunication engineering. His research interests include smart sensors, the Internet of Things, digital signal processing, and FPGA-based artificial intelligence.

Noman Mustafa is a software developer for INTAC Optical Instruments Co., Ltd, China. He received his MS in Electronics and Communication Engineering in 2020 from Shanghai Jiao Tong University. For his master's degree, he received a fully-funded scholarship from the Chinese Scholarship Council. His research interests include IoT, Micro-Defect Detection, and Deep Learning. His recent industrial experience includes developing a complete defect detection system for a number of Chinese industrial manufacturing plants.

Abdelwahed Nahli is a PhD candidate at Fudan University, Shanghai as well as a research fellow at the Shanghai Institute for pattern recognition and data science. In 2015, he obtained his BS in computer engineering from Hassan II University, Casablanca. In 2021, he earned his MS in information and communication engineering from Shanghai University, Shanghai. His research interests are the internet of things, computer vision, artificial intelligence and data science.

Dr. Saadullah Farooq Abbasi is an Assistant Professor in the Department of Biomedical Engineering at Riphah International University Islamabad, Pakistan. He has completed his PhD from Fudan university, Shanghai, China. His research interests are IoT, health informatics, sleep, EEG signal processing.

Abdulhamit Subasi is specialized in Artificial Intelligence, Machine Learning, Biomedical Signal/Image Analysis, and security. Concerning the application of Artificial Intelligence/Machine Learning to different fields, he wrote more than 40 book chapters and more than 220 published journal and conference papers. He is the series editor of "Artificial Intelligence Applications in Healthcare & Medicine". He is also the author of the books, "Practical Guide for Biomedical Signals Analysis Using Machine Learning Techniques", "Practical Machine Learning for Data Analysis Using Python" and the editor of the books "Applications of Artificial Intelligence in Medical Imaging" and "Advances in Non-Invasive Biomedical Signal Sensing and Processing with Machine Learning". He worked at many institutions as an academician and at Georgia Institute of Technology, Georgia, USA, as a researcher. He has been awarded the Queen Effat Award for Excellence in Research, in May 2018. He worked as a professor of computer science at Effat University, Jeddah, Saudi Arabia between 2015 and 2020. Since 2020, he has been working as a Professor at the Faculty of Medicine, University of Turku, Turku, Finland.

Tomi Westerlund (Senior Member, IEEE) is a Professor of Robotics and Autonomous Systems with the University of Turku. He leads the Turku Intelligent Embedded and Robotic Systems Research Group (tiers.utu.fi), University of Turku, Finland. His current research interest is in the areas of Industrial IoT, smart cities and autonomous vehicles (aerial, ground, and surface), and (co-)robots. In all these application areas, the core research interests include energy efficiency, dependability, interoperability, fog/edge computing, and edge AI.

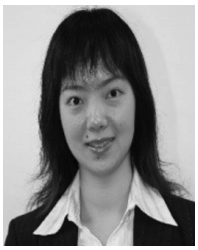

Wei Chen (Senior Member, IEEE) received the B.Eng. and M.Eng. degrees from the School of Electronics and Information Engineering, Xian Jiao Tong University, China, in 1999 and 2002, respectively, and the Ph.D. degree from the Department of Electrical and Electronics Engineering, The University of Melbourne, Australia, in 2007. She worked as an Intern with Bell Laboratories, Germany, Alcatel-Lucent, Stuttgart, in 2005, and she was a Research Assistant with the Department of Electrical and Electronics Engineering, The University of Melbourne in 2007. From 2007 to 2015, she was an Assistant Professor with the Eindhoven University of Technology, The Netherlands. From 2009 to 2013, she served as the Chair of Theme Health Care with the Department of Industrial Design, Eindhoven University of Technology. Since October 2015, she has been a Full Professor and the Director of the Center for Intelligent Medical Electronics (CIME), Department of Electronic Engineering, School of Information Science and Technology, Fudan University. Her research interests include patient health monitoring, medical monitoring system design using wearable sensors, sleep monitoring, brain activity monitoring, wireless body area networks, ambient intelligence, personalized and smart environment, smart sensor systems, and signal processing. She is an Associate Editor of IEEE Transactions on Neural Systems and Rehabilitation Engineering (TNSRE) and IEEE Journal on Biomedical Health Informatics (JBHI), and a Managing Editor of IEEE Reviews in Biomedical Engineering (R-BME).